

Data Quality Report - 2016

Hyperspectral

ARSF - Data Analysis Node

Updated on: April 12, 2016

Contents

1	Introduction	2
2	Geo-referencing accuracy	2
3	Timing Errors	3
4	Sensor calibration	4
4.1	Wavelength calibration accuracy	4
4.2	Radiometric calibration accuracy	4
5	Pixel Overflows	8
6	Bad CCD Pixels	8
6.1	Detection method A - Constant input variable output (CIVO)	10
6.2	Detection method B - Constant input constant invalid output (CICO)	10
6.3	Detection method C - Linear input non-linear output (LINO)	11
6.4	Detection method D - Rapid saturation	11
6.5	Detection method E - Visual inspection	12
6.6	Detection method F - Detector sensitivity	12

1 Introduction

The Airborne Research and Survey Facility (ARSF) collect hyperspectral data with a Specim AISA Fenix instrument, operated since 2014. The Fenix instrument comprises two detectors covering the Visible to Near Infra-Red (VNIR) and Short Wave Infra-Red (SWIR) regions, giving a total spectral range of 380–2500 nm. It replaced the Eagle (400–970 nm) and Hawk (970–2500 nm) hyperspectral instruments previously operated by ARSF. This data quality report describes issues for hyperspectral data acquired with the Fenix instrument that should be considered when further processing any ARSF datasets acquired from 1st January 2016 until the start date listed in the succeeding data quality report.

This document may be updated over the course of the year, the latest version is available at:

<https://arsf-dan.nerc.ac.uk/trac/wiki/Reports>

2 Geo-referencing accuracy

ARSF currently delivers level 1b (calibrated at-sensor radiance) and level 3 data (mapped level 1b data). This offers users quick access to georeferenced data whilst maintaining the capability to operate on the original pre-gridded data and use a coordinate projection or datum of choice.

The quality of the geocorrection for each project is described in the documentation supplied with the delivery. Typically the geocorrection is of the order of a couple of metres, equating to approximately 1 pixel depending on flight altitude. High accuracy relies on an accurate Digital Surface Model (DSM). The freely available global ASTER digital elevation data are used during quality checks and an elevation model is supplied with the delivered mapped files. Accuracy may be improved by using a DSM derived from higher resolution data such as LiDAR. An indication of the average error between vector overlays is included in the delivery documentation where vector overlays or other ground truth information is available.

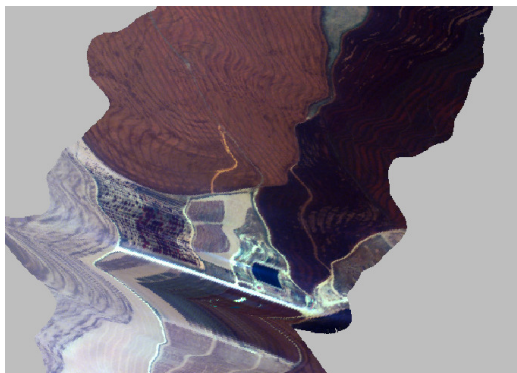
It may be possible to tune specific flight lines for higher accuracy and instructions can be provided on how to make your own alignments. If a higher accuracy is required, please contact us at: arsf-processing@pml.ac.uk

3 Timing Errors

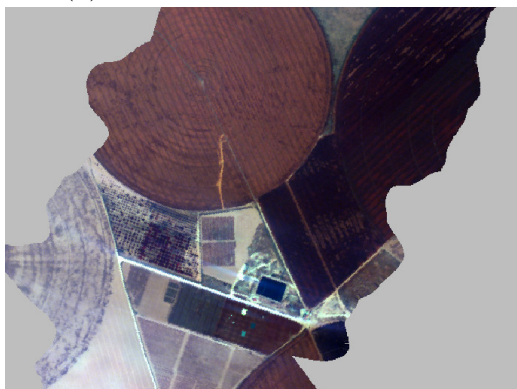
Small timing errors occur due to a fault in synchronisation between the navigation system and the Specim sensors. For the Fenix instrument these errors vary for each flight but average $0.9 \text{ s} \pm 0.3 \text{ s}$. These timing offsets result in an incorrect scan line position, which manifest as distortions in the imagery. These distortions correlate to movements of the aircraft, but are out of sync. An example is shown in Figure 1.

This issue has been extensively investigated and demonstrated to be a fault in the Specim systems. ARSF are working with Specim to resolve this issue.

We endeavour to correct all timing errors prior to delivery. As this is a manual process reliant on finding suitable visible features in the imagery some errors may still remain. If any are found please contact us at arsf-processing@pml.ac.uk.



(a) *Timing error in a flightline.*



(b) *Corrected version of the above image (0.5 s timing difference).*

Figure 1: *Illustration of timing offset present in geo-referenced Fenix data.*

4 Sensor calibration

The Fenix sensor calibration is undertaken annually in collaboration with the NERC Field Spectroscopy Facility to ensure spectral (wavelength) and radiometric accuracy. The calibration event in February 2016, undertaken at the British Antarctic Survey's facilities in Cambridge, covers all flights from January 2016 until present.

4.1 Wavelength calibration accuracy

Wavelength calibration is performed by collecting data from a range of spectral lamps. These lamps provide spectral emission features at known wavelengths that can be detected with the Fenix sensor. This procedure allows specific pixel numbers to be checked against known wavelengths. The lamps included in the calibration were: Mercury-Argon (Hg-Ar), Hydrogen (H), Helium (He), Oxygen (O), Neon (Ne), Xenon (Xe) and Krypton (Kr). Differences from known spectral features versus their values measured by the Fenix can be found in Table 1 (VNIR) and Table 2 (SWIR). There are many more spectral lines identified for the VNIR region as there are many more distinct emission lines for each lamp in the VNIR region than the SWIR. ARSF plan to investigate whether there are more reliable spectral emission lines that can be used for the SWIR region to increase the confidence in the SWIR wavelength calibration.

The Full Width at Half Maximum (FWHM) values in these tables have been obtained by fitting Gaussian curves to the spectral features and then measuring the FWHM for the best-fitting curve. While this procedure gives a reasonable estimate of the FWHM values, some caution is recommended for applications relying on accurate FWHM values. Note that the FWHM as labelled in the data header (.hdr) files is the bandwidth of each band.

4.2 Radiometric calibration accuracy

Radiometric calibration was undertaken on the Fenix instrument using an integrating sphere provided by the NERC Field Spectroscopy Facility. The sphere was calibrated in accordance with National Physics Laboratory Standards and a light source of known radiance was provided at each wavelength in use. This procedure allows a radiometric calibration curve to be obtained for the Fenix.

Spectral Line (nm)	Measured Wavelength (nm)	FWHM (nm)	Error (nm)	Pass/Fail (<2nm Err.)
404.7	405.10	4.32	-0.40	Pass
435.8	436.19	2.79	-0.39	Pass
486.1	486.45	2.96	-0.35	Pass
501.6	501.93	3.17	-0.33	Pass
546.1	546.21	2.72	-0.11	Pass
578.1	578.18	4.56	-0.08	Pass
594.4	594.74	2.93	-0.34	Pass
607.9	609.10	4.07	-1.20	Pass
656.3	656.31	3.33	-0.01	Pass
667.8	667.95	3.46	-0.15	Pass
692.9	693.19	3.43	-0.29	Pass
706.7	706.85	3.62	-0.15	Pass
717.4	717.90	3.83	-0.50	Pass
728.1	728.42	4.04	-0.32	Pass
738.4	738.66	3.38	-0.26	Pass
750.9	751.10	3.76	-0.20	Pass
763.5	763.79	3.55	-0.29	Pass
785.5	785.71	3.56	-0.21	Pass
801.1	801.41	3.49	-0.31	Pass
811.1	811.45	3.49	-0.35	Pass
823.2	823.45	3.38	-0.29	Pass
837.8	838.22	3.37	-0.42	Pass
849.5	849.82	2.81	-0.32	Pass
878.2	877.97	3.03	0.23	Pass
892.9	893.16	2.97	-0.26	Pass
Mean		3.44	-0.29	

Table 1: *VNIR Wavelength calibration offsets for the February 2016 calibration of the Fenix.*

Spectral Line (nm)	Measured Wavelength (nm)	FWHM (nm)	Error (nm)	Pass/Fail (<2nm Err.)
1083	1083.05	10.98	-0.05	Pass
1363.4	1364.69	15.21	-1.27	Pass
1816.7	1816.48	12.03	0.25	Pass
2058.7	2057.64	10.98	1.06	Pass
Mean		12.3	0.003	

Table 2: *SWIR Wavelength calibration offsets for the February 2016 calibration of the Fenix.*

Radiometric calibration has been performed on the ARSF Fenix on four separate occasions: December 2013, February 2014, February 2015 and February 2016. The sensor was found to be radiometrically stable over the 2013–2014 period with an average change of 0.15 %. Between the February 2014 and February 2015 calibrations a change of 3.24 % was found, and between the February 2015 and February 2016 calibrations there was a change of 0.42 %. The large shift between the 2014 and 2015 calibrations is thought to be due to extreme environmental conditions during the Malaysia campaign (September–November 2014). An examination of the water absorption features in the SWIR wavelengths for these data highlighted the instability. No further instability in the sensor has been observed since the 2015 calibration.

A graph displaying the change between the two calibrations is shown in Figure 2. The regions displaying larger changes are mainly restricted to the edge of the detectors, where the bands have the lowest sensitivity and poorest performance. The region around band 348 corresponds to the edge between the VNIR and SWIR detectors.

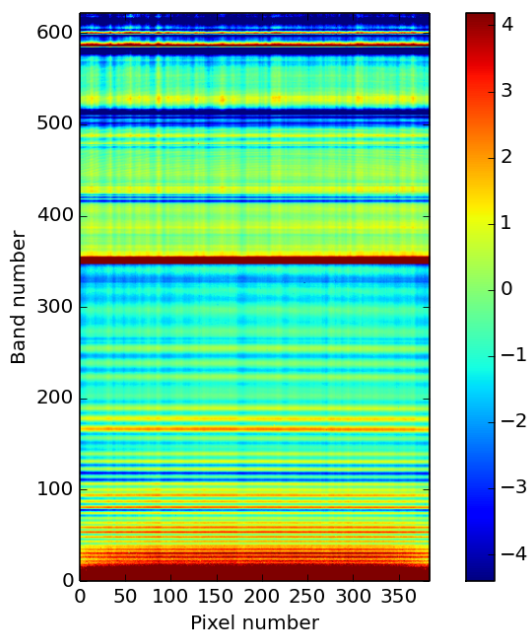


Figure 2: *Fenix* calibration multiplier percentage differences between February 2015 and February 2016 calibrations. The region around band 348 corresponding to the edge between the VNIR and SWIR detectors is clearly visible with the larger than average shift.

5 Pixel Overflows

Hyperspectral instruments have a finite dynamic range and must be configured to capture data such that the received signal strength falls within this range. For example, if the area of interest is dark, then the instrument will be configured to capture as much low light as possible. Configuration of the Fenix instrument is set based on operator experience, prevailing conditions and the requested principal investigator's areas of importance. Inevitably some pixels are unexpectedly bright due to high responses recorded on the instrument, such as sunglint over water or reflected light from part of a cloud. These pixels may exceed the maximum capture level and 'overflow'. These pixels are not typically in areas of interest but should be accounted for when examining files. The accompanying mask file will contain an overflow flag value in the level 1 equivalent pixel. If you would prefer your actual level 1 files to be masked rather than use the separate mask file, please contact arsf-processing@pml.ac.uk.

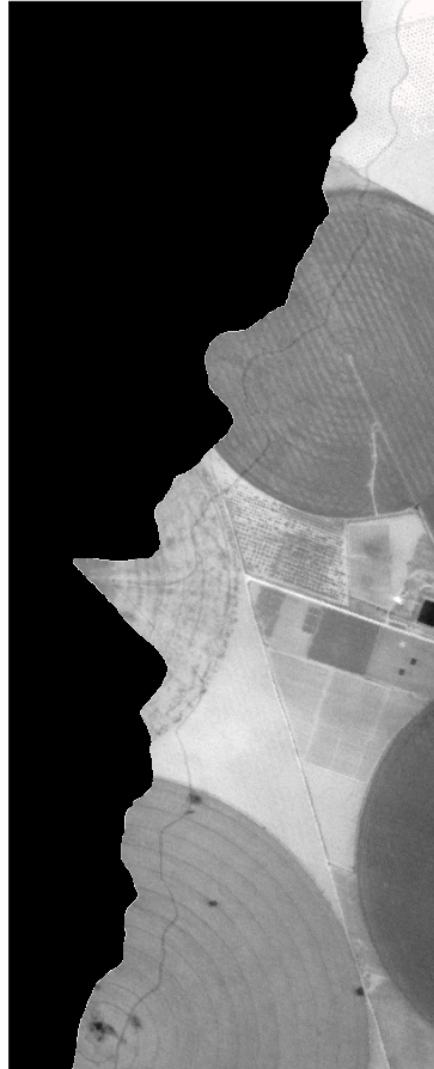
6 Bad CCD Pixels

The Fenix instrument has a varying number of pixels that provide inaccurate values, these are identified and flagged as 'bad pixels' during calibration. A list of known bad pixels has been included in the mask files supplied with processed data. Based on the type of Charge-Coupled Device camera used in the Fenix instrument $\sim 1\%$ of pixels (about 600) are expected to be bad. Bad pixels manifest in level 1 datasets as straight lines along the direction of flight and appear as undulating lines following the motion of the aircraft in level 3 data. An example is shown in Figure 3. Typically bad pixels will only affect a single wavelength band making detection difficult. A complete solution for identification and removal of bad pixels from the Fenix instrument was finalised in 2014 and is updated every year.

The final list of bad pixels uses six methods of detection that are executed on a set of test data. If a test fails for a particular pixel then that pixel will be flagged with that failure method. A flag is recorded for each test failed by that pixel, possibly resulting in multiple failure flags that are summed together. Masking of only certain bad pixel types is possible using the failure flags written to the mask file.



Level 1



Level 3

Figure 3: *Bad pixel on one Fenix band. On the left, bad pixel appears as a straight line in level 1 data; on the right, the same one is visible in level 3 as an undulating line.*

6.1 Detection method A - Constant input variable output (CIVO)

The CIVO method identifies pixels as bad pixels when they vary significantly given a constant light source as input. This is performed by considering the median raw value or Digital Number (DN) for the pixel over time, and testing individual epochs against a percentage threshold. If the value exceeds the threshold then the pixel is flagged as bad.

6.2 Detection method B - Constant input constant invalid output (CICO)

The CICO method identifies bad pixels when their response to a constant light greatly varies from the response of their spatial and/or spectral neighbours. As with the previous method the procedure is applied to raw values. To determine when a pixel's response varies it must be compared to its nearest neighbours.

To detect responses that differ significantly the mean and standard deviation of values are calculated for a moving window. These values are then used in the formula below.

$$B = \frac{\mu_c - \mu_{(s,b)}}{\sigma_{(s,b)}} \quad (1)$$

where μ_c is the mean of the CCD and $\mu_{(s,b)}$ and $\sigma_{(s,b)}$ are the mean and standard deviation over a window centred on sample s and band b . When B exceeds the threshold, the bad-counter for this pixel is incremented. Once the counter reaches the maximum allowed value, the pixel being tested is selected as bad.

6.3 Detection method C - Linear input non-linear output (LINO)

The LINO method takes the average DN for each pixel over time for multiple data captured at increasing integration times. Increasing integration time should have a direct linear sensor response for every pixel. Using regression over the average values versus integration time it is possible to get a measurement of linearity using the Pearson Correlation Coefficient (r). The closer r is to 1.0 the better the linear regression. The formula is given as:

$$r = \frac{\sum_{i=1}^N [(t_i - \bar{t})(d_i - \bar{d})]}{\sqrt{\sum_{i=1}^N [(t_i - \bar{t})^2] \sum_{i=1}^N [(d_i - \bar{d})^2]}} \quad (2)$$

where t is the integration time, d the mean DN for each pixel and \bar{t} and \bar{d} their means over the number of pixels tested (N). A pixel is flagged as bad if r is less than the threshold value.

6.4 Detection method D - Rapid saturation

The rapid saturation detection identifies a bad pixel if it is saturating more rapidly than its neighbours. This method works similarly to CICO to detect linear but invalid responses for different integration times. It compares the coefficients of the linear regression of mean pixel values versus integration times. As the previous method, a moving window of fixed spatial and spectral width will iterate over each pixel of each band. If the slope at the centre of the window being tested varies greatly in relation to its neighbours, then the pixel in that position will be flagged as a bad pixel. The function used to scan over each pixel is:

$$D = \frac{b_c - \mu_{(s,b)}}{\sigma_{(s,b)}} \quad (3)$$

where, μ and σ are the mean and standard deviation and b_c is the slope of the CCD pixel given by a general regression:

$$Y = a + b_c X \quad (4)$$

If D exceeds the threshold, then the pixel will be classified as bad.

6.5 Detection method E - Visual inspection

The visual inspection method consists of an extensive examination using in-house software. Pixels identified by an experienced analyst as giving erroneous results are selected as bad pixels. Erroneous results are identified by comparing those pixels with their neighbours. If a pixel is consistently brighter or darker than its closest pixels, it is marked as a bad pixel.

6.6 Detection method F - Detector sensitivity

The detector response is non-uniform across each of the bands. The lowest sensitivity is found in bands at the upper and lower limits of each detector. These bands have high calibration gains and noisy data may result in spikes in the radiometrically calibrated data. The normalised sensitivity (sensitivity for each band divided by maximum sensitivity for detector) is calculated, as shown in Figure 4. Bands with a sensitivity lower than a given threshold are marked as bad. Thresholds of <10 % and <30 % are used to mask out bands in the VNIR and SWIR regions respectively. Separate thresholds are used for the VNIR and SWIR regions due to the different characteristics of each detector.

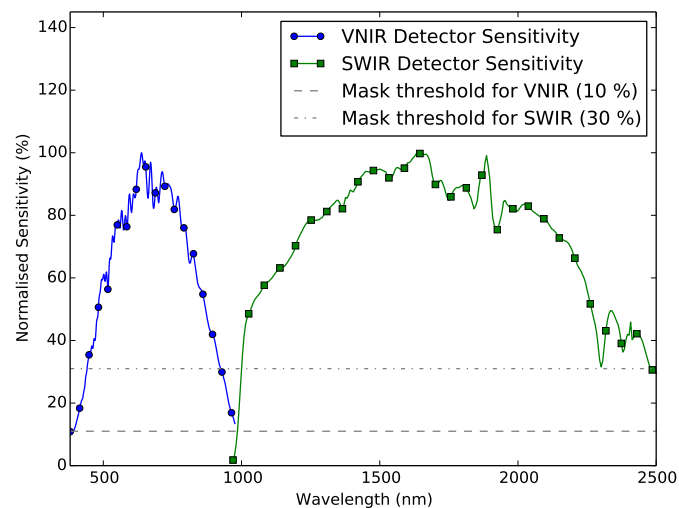


Figure 4: *Normalised sensitivity of the VNIR and SWIR bands for Fenix detector.*